

PHYSICS INVESTIGATION

Correlation between small-volume spinal cord doses for spine stereotactic body radiotherapy (SBRT)

Lijun Ma, PhD¹, Lei Wang, PhD², Young Lee, PhD³, Chia-Lin Tseng, MDCM³, Scott Soltys, MD², Steve Braunstein, MD, PhD¹ and Arjun Sahgal MD³

¹Department of Radiation Oncology, University of California San Francisco, San Francisco, CA, USA

²Department of Radiation Oncology, Stanford University, Stanford, CA, USA

³Department of Radiation Oncology, Sunnybrook Odette Cancer Centre, University of Toronto, Toronto, ON, Canada

Correspondence to: Lijun Ma, PhD, FAAPM, Department of Radiation Oncology, University of California San Francisco, 505 Parnassus Avenue, San Francisco, CA 94143, USA; Email: lijun.ma@ucsf.edu

(Received: February 14, 2018; Accepted: May 2, 2018)

ABSTRACT

Purpose: Doses to small spinal cord isodose volume (such as those ranging from Dmax 0.0 cc to 0.5 cc) as well as to large volumes (such as those ranging from 0.5 cc to 3.0 cc) are critical parameters to guide safe practice of spine SBRT. We here report a mathematical formula that links the most probable dose volume limits together for common spine SBRT cases.

Methods and materials: A dose ripple formula parameterized with equivalent dose radius (EDR) was derived to model spinal cord small-volume doses for a spine SBRT treatment. A cohort of spine SBRT cases (n=68), treated with either a robotic x-band linac or a conventional S-band linac, was selected to verify the model predictions. The mean prescription dose was 22± 4 Gy (range, 12-40 Gy) delivered in 2±1 fractions. The mean and median target volume was 39.4±42.5 cc and 30.3 cc (range, 0.24-264.2 cc), respectively. Direct correlations between the spinal cord Dmax and variable spinal cord doses of increasing isodose volumes (ranging from 0.0 cc to 3.0 cc) of different planning organ-at-risk volumes (PRVs) were investigated. The PRV structures for the study included the true cord, thecal sac and the true cord plus variable margins ranging from 1.0 mm to 3.0 mm.

Results: No direct linear correlation was observed amongst the small volume doses to the spinal cord PRVs. However, strong linear correlations ($R^2 > 0.96$) for all the studied PRVs were observed when correlating EDRs amongst isodose volumes ranging from 0.0 cc to 3.0 cc. In particular, EDR dependence was found to differ significantly for the thecal sac versus the spinal cord with or without 1-3 millimeter margins. With strong EDR correlation, the most probable relationship among the small-volume dose limits was derived for the spinal cord PRVs.

Conclusion: An analytical formula linked the most probable pin-point/small isodose volume doses with relatively large isodose volume doses of the spinal cord for spine SBRT. As a result, a small number of dose limits such as Dmax or D(0.35cc) are likely sufficient to surrogate the spinal cord dose tolerance for consistent treatment planning optimization and outcome analysis.

Keywords: spinal cord, dose ripple effect, stereotactic body radiotherapy, dose volume limits

INTRODUCTION

Spine stereotactic body radiation therapy (SBRT) has been rapidly expanding in de novo and re-irradiation settings with respect to both metastatic and benign tumors [1-8]. One of the key challenges of spine SBRT is to maximally spare the spinal cord, which is often adjacent to the planning target volume (PTV). In most cases, a sharp dose fall-off is demanded from the target across the spinal cord in order to achieve optimal sparing [9-11]. This leads to a significantly inhomogeneous dose deposition within the spinal cord volume, which results in large variations between the point maximum dose (Dmax) and the doses encompassing finite hot-spot isodose volumes such as D(0.1 cc) to D(1.0 cc) [12]. Various approaches of limiting spinal cord dose have thus been reported for treatment planning optimization as well as outcome analysis[13].

Some multi-institutional studies have adopted the thecal sac as a surrogate for the planning-organ-at-risk volume (PRV) [5, 9, 11, 14, 15]. Other studies have adopted dose to small isodose volumes (for example, D(0.1 cc) or D(0.35 cc) of the true spinal cord with no PRV as the critical dose volume limits [16-18]. The question arises as to whether a single or a few number of dose-volume limits would be sufficient to surrogate the full spinal cord dose tolerance. In particular, a large volume of the spinal cord may receive a significant dose during treatment; there is uncertainty in how to specify other dose-volume limits such as doses to 0.35 cc, 1.0 cc, and 2.0 cc without causing conflictive and/or suboptimal treatments.

The fundamental question to these concerns is whether the most probable dose volume limits of small volume irradiation (such as Dmax or D(0.35 cc)) can be linked to relatively large volume irradiation (such as D(0.5 cc) or D(1.0 cc) etc.). The goal of this study is therefore to investigate whether such a relationship exists, and if so, its correlative power as well as its mathematical expression and implication on the PRV selections.

MATERIALS AND METHODS

Modern spine SBRT treatments are predominantly administered with the robotic X-band linear accelera-

tor (i.e., CyberKnife SBRT) or the conventional S-band linear accelerator (i.e. Linac-based SBRT)[7, 18, 19]. For the current study, a cohort of 68 patients treated with spine SBRT were randomly selected and analyzed (n = 42 for linac-based SBRT and n = 26 patients for CyberKnife SBRT). A mean dose of 22 ± 4 Gy (ranging 12-40 Gy) in 2 ± 1 fractions (ranging from 1 to 5) was prescribed for the studied cases. The mean prescription isodose value was $87.7 \pm 9.7\%$. The prescription isodose volume (encompassed at least 95% of the target volume) was 51.2 ± 50.8 cc (range 0.4 cc to 298.4 cc), and the planning target volume was 39.4 ± 42.5 cc with contoured thecal sac volume of 18.8 ± 43.3 cc (range 4.4 cc to 68.1 cc).

The spinal cords for all the cases were located in the vicinity of the PTV in the peripheral dose fall-off region. The thecal sac was investigated first as the volume of reference for the current study based on the previous publication [15]. Subsequently, true cord and variable margin-expanded (e.g. 1 mm, 2 mm and 3 mm margins) cord volumes were obtained and analyzed for comparisons.

Both robotic and linac-based SBRT treatment techniques of our institutions have been extensively reported in the literature[9, 16, 20, 21]. In short, robotic treatments used near real-time 2D stereoscopic imaging to guide treatment setups and the treatment utilized 100 to 300 non-isocentric beams to produce a conformal dose distribution surrounding a target volume. In contrast, linac-based spine SBRT treatments primarily apply 3D volumetric cone-beam CT imaging coupled with a rigid body fixation device for treatment setups. The delivery of linac-based SBRT used either fixed intensity modulated or rotational volume modulated arc beams.

To determine the most probable relationship among the small-volume PRV dose limits for a spine SBRT treatment, we introduced an Equivalent Dose Radius (EDR) to convert a non-uniform expanding isodose surfaces from a target to concentric expanding dose surfaces similar to a ripple radiation. The EDR is defined as follows,

$$EDR \equiv k [V(D)]^{1/3} \quad (1)$$

where V is a peripheral isodose volume surrounding an irradiated target volume for a given dose level D [22], and k is a constant dependent on the shape of the target. For example, $k = (3/(4\pi))^{1/3} = 0.6$ for a spherical volume and $k = (1/(n\pi))^{1/3}$ for a cylindrical volume, where n is a scaling factor given as the ratio of its length and base radius (Figure 1). Despite variable k values, if we normalize EDR with a reference EDR_0 , then the dependence of k is eliminated.

Furthermore, if a reference EDR_0 is taken as the equivalent dose radius for isodose volume (V_0) at the dose of (D_0), then Equation (1) for the most probable EDR and D values can be rendered as

$$\begin{aligned} EDR &\equiv EDR_0 [V(D)/V(D_0)]^{1/3} \\ &= EDR_0 [D/D_0]^{\gamma/3} \end{aligned} \tag{2}$$

In the second step of Equation 2, general mean dose fall-off model of our previous publication[22] was applied, i.e., the peripheral isodose volume V(D) and its corresponding isodose level D is described as follows,

$$V(D)/V(D_0) = [D/D_0]^{\gamma} \tag{3}$$

where $\gamma \neq 0$ is an empirical parameter. In the above derivations of Equation 2 and 3, it is assumed that the spinal cord is located in the peripheral dose fall-off region of the target without overlaps. For such cases, $\gamma = -1.5$ (i.e. $\lambda = 2$) following the inverse square law from the previous publication [22].

Furthermore, if we let the small-volume dose (D) inside the PRV correspond to the peripheral isodose surface of the same value (For example, if $D_{max} = 14$ Gy for the spinal cord PRV, then EDR_{max} would correspond to the 14-Gy isodose volume, and if $D(0.1 \text{ cc}) = 13$ Gy, then $EDR(0.1 \text{ cc})$ would correspond to the 13-Gy isodose volume, etc.), and we can further substitute $EDR_0 = EDR_{max}$ and $D_0 = D_{max}$ and solving for EDR/EDR_{max} via Equation 2, then we have ,

$$D_{max} = D \times [EDR / EDR_{max}]^{\lambda} \tag{4}$$

where λ is a fixed parameter, i.e., $\lambda = -3/\gamma$. Note that if the most probable EDR/EDR_{max} value can be reliably estimated from the mean EDR/EDR_{max} value over the studied cases, then the most probable D versus D_{max} relationship would be also established.

For the current study, EDRs of variable isodose volumes (from EDR_{max} to $EDR(3 \text{ cc})$) of the spinal cord

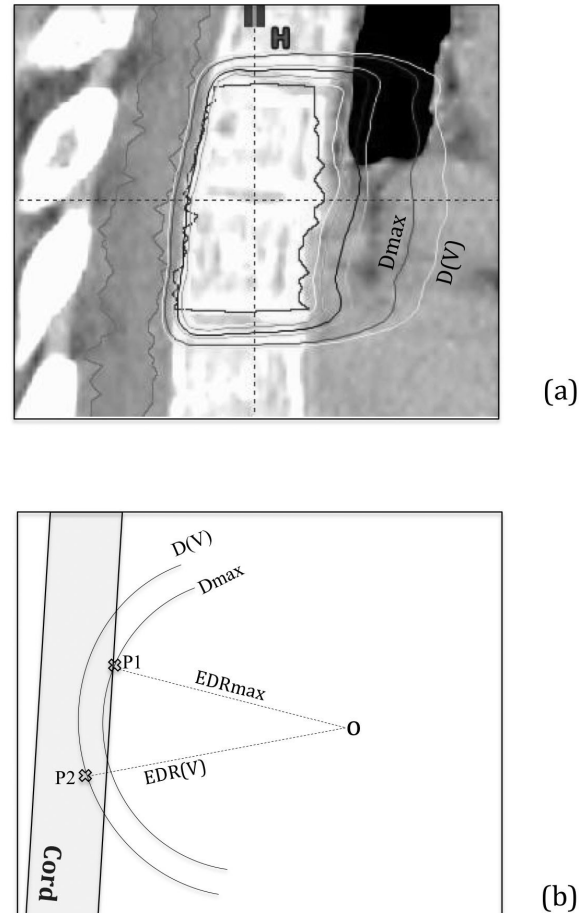


Figure 1. Schematic illustration of the EDR definition: (a) shows a clinical case with the peripheral isodose surface corresponds to the spinal cord D_{max} value and another corresponds to small-volume $D(V)$ such as $D(0.3 \text{ cc})$ etc. and (b) illustrates the corresponding EDR parameters including D_{max} of the spinal cord for the case.

PRVs (e.g., thecal sac, cord, cord plus 1 mm to 3 mm margin) were extracted and computed for each case. Dose and EDR values at finite volumes (ranging from 0.1 cc to 3.0 cc) for all structures were fitted via linear regression analysis. The goodness of the fit and confidence intervals on the fitting parameters were analyzed for thecal sac, cord and cord with expanded margins for 1 mm to 3 mm.

RESULTS

Figure 2 shows the direct correlation results for the thecal sac point D_{max} versus doses at variable

hot-spot isodose volumes. Note that $D_{max} = D(0 \text{ cc})$ by definition. As shown in Figure 2, $D(0.1 \text{ cc})$ or smaller volume dose parameters correlated somewhat with the D_{max} due to near neighborhood approximation. However, such an effect degraded rapidly with increasing isodose volumes. For example, $R^2 = 0.918, 0.796, 0.711, 0.522$ for $D(0.1 \text{ cc}), D(0.5 \text{ cc}), D(1.0 \text{ cc})$ and $D(3.0 \text{ cc})$, respectively. Both Linac-based and Cyberknife cases (except some outliers) followed similar trend of dependence as shown in Figure 2. As a result, direct linear correlation could not be used to estimate the most probable small-volume dose limits from the studied cases.

In contrast, strong EDR correlation ($R^2 > 0.96$) across the isodose volumes from EDR(0.0 cc) or EDRmax (the maximum dose point) up to EDR(3.0

cc) as shown in Figure 3. Furthermore, the slope (S) of the fitted line increases with increasing isodose volumes. Based on the mean S values, the most probable D_{max} versus D relationship was derived via Equation 4. No statistically significant difference in the slope values was detected via t-scores between the robotic Cyberknife and conventional linac treated cases for all the isodose volumes, e.g., $p = 0.20, 0.40, 0.45, 0.92$ corresponding to EDR(0.1 cc), EDR(0.5 cc), EDR(1.0 cc) and EDR(3.0 cc), respectively.

In addition, EDR correlations were similarly observed for the cord and PRVs consisting the cord plus 1 to 3 mm margins. This is illustrated in Figure 4, where EDR(1.0 cc)/EDRmax value is shown for the cord plus 1-3 mm margin respectively. Note that the mean

Thecal Sac Dose(Gy) Correlation

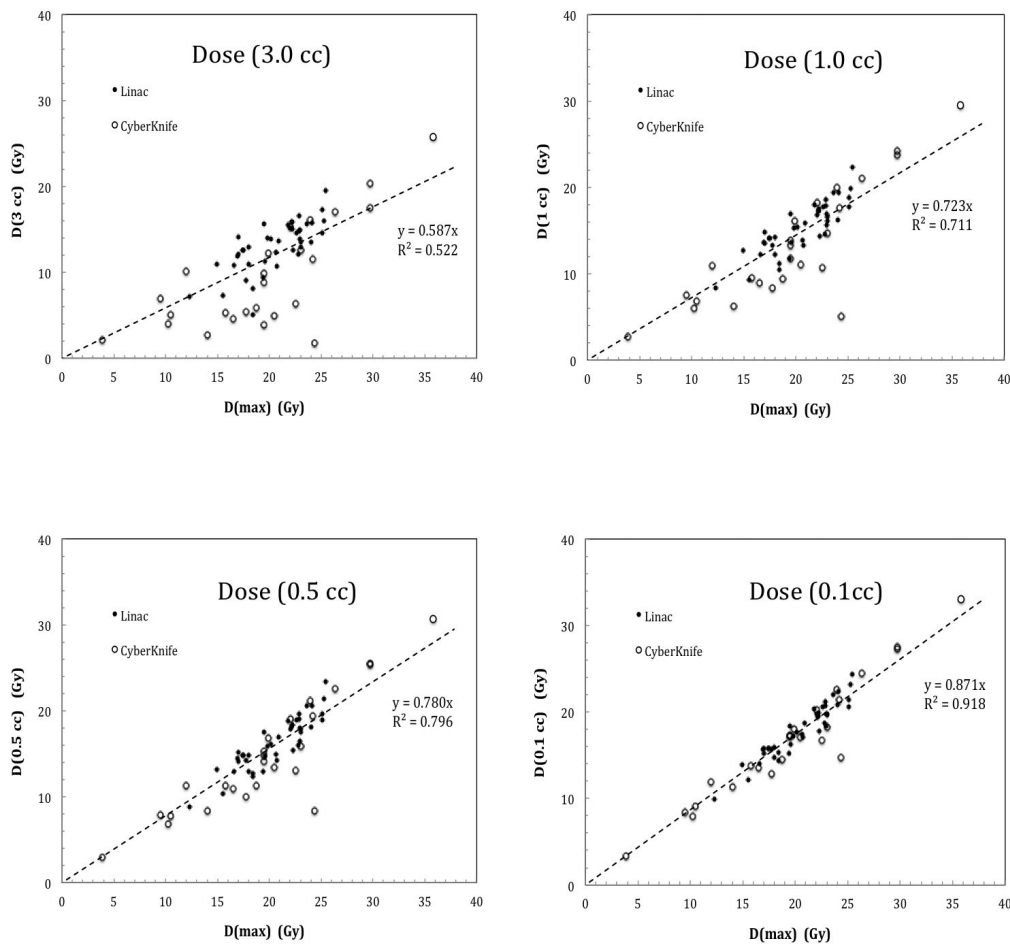


Figure 2. Dose correlation results for the thecal sac at variable isodose volumes from 0.1 cc to 3.0 cc. Relatively strong correlation ($R^2=0.918$) was observed for small isodose volume such as 0.1 cc due to the near-neighborhood effect while significantly weaker correlation was seen for large isodose volumes such as $R^2=0.522$ at 3.0 cc instead.

EDR(V) vs EDR(max) for the Thecal Sac

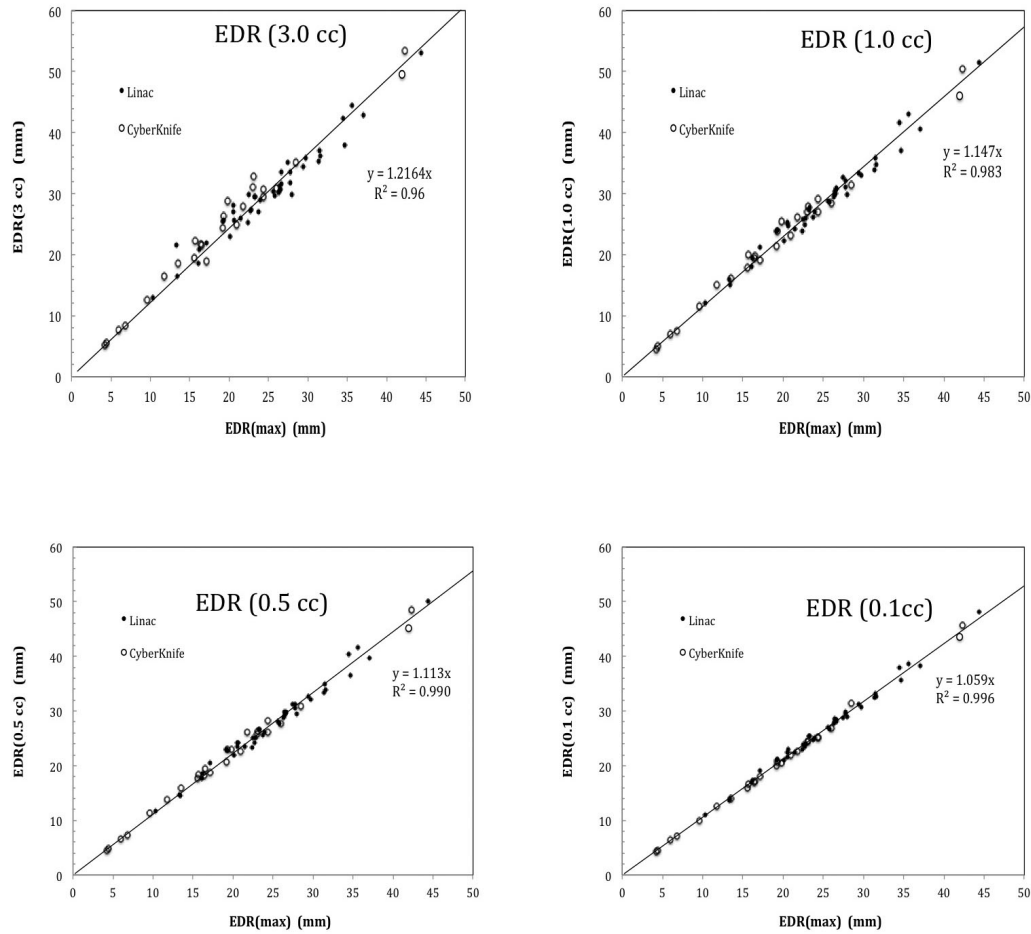


Figure 3. EDR correlation results at variable isodose volumes ranging from 0.1 cc to 3.0 cc. Note that a strong correlation with $R^2 > 0.98$ was observed for isodose volumes up to 1.0 cc regardless Cyberknife or linac-based treatments.

EDR(1.0 cc)/EDRmax agreed excellently for variable margin sizes.

Figure 5 further summarizes the dependence of the EDR/EDRmax ratio for different PRV definitions. Note the large discrepancies between the thecal sac and the cord and cord-related PRVs in Figure 5. This suggests that thecal sac cannot be simply equated to the true cord plus a uniform margin for simple dose volume limits applications.

DISCUSSION

A mathematical formula was found to strongly link the most probable adjacent spinal cord doses from the

Dmax to variable volumetric parameters ranging from D(0.1cc) to D(3.0cc). The fitted model was found applicable to variable dose fractionation schemes and different treatment modalities, i.e., robotic CyberKnife SBRT and linac-based SBRT.

At the isodose level of up to 1.0 cc, a strong EDR correlation ($R^2 > 0.98$) was surprisingly observed for all the PRV values. Such a correlation enables a user to empirically convert the small-volume dose limits to different spinal cord PRVs via Equation 4 and Figure 5. For example, a dose of 10 Gy to 0.35 cc of the cord would correspond to a Dmax dose of 12 Gy. This can be calculated by first obtaining $EDR(0.35cc)/EDRmax = 1.075$ from Figure 5, and then by applying Equation 4 such that $Dmax = 10 * (1.075)^2 = 12$ Gy.

EDR(1.0 cc)/EDR(max) For Cord PRVs

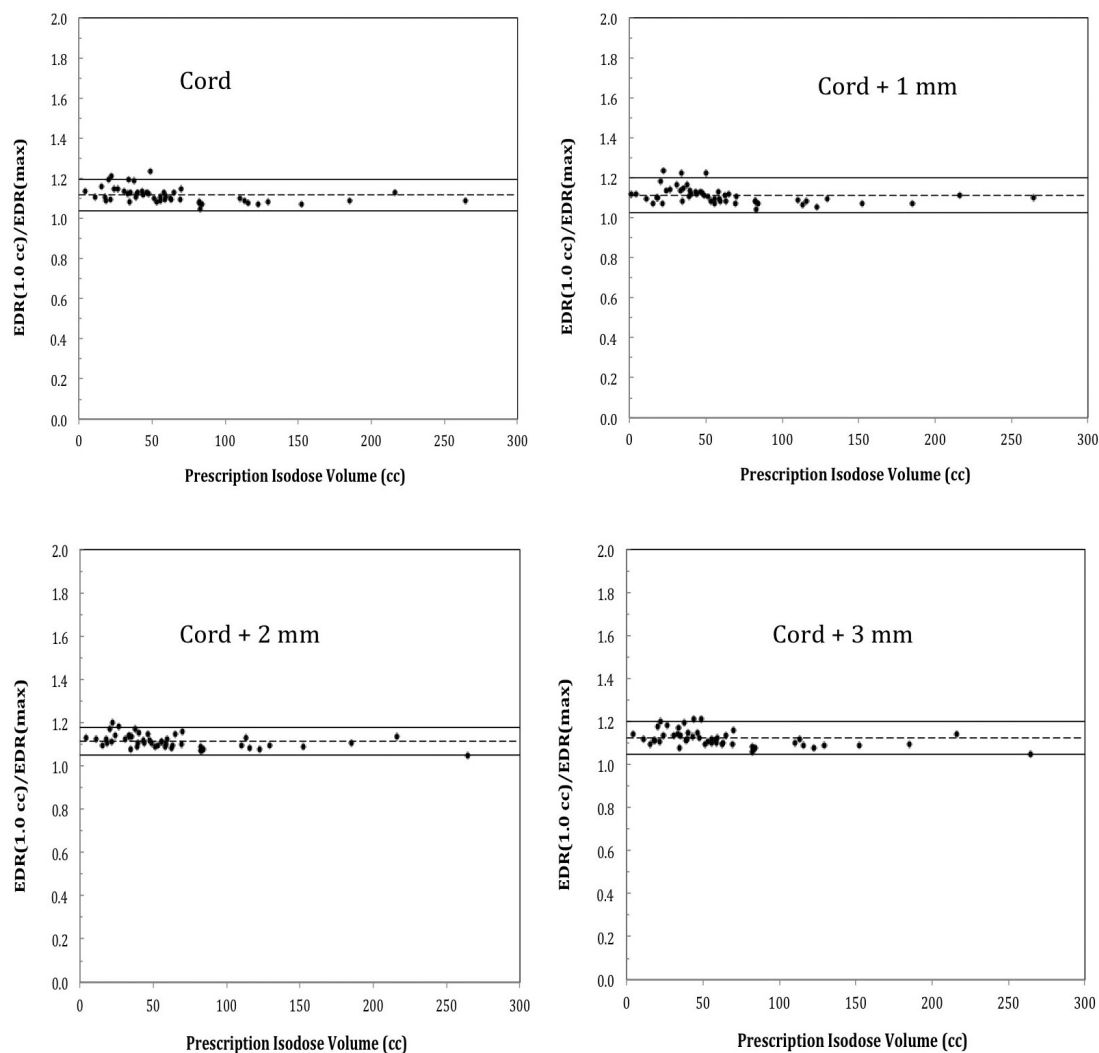


Figure 4. Plots of EDR(1.0 cc)/EDR(max) ratio for the true cord and true cord plus 1 mm to 3 mm margin without assuming linear correlation of all the parameters.

Our study has also shown that adopting consistent PRV definitions is critical when imposing the spinal cord dose volume limits or cross-comparing treatment outcome. For example, the thecal sac PRV does not approximate the true cord plus a PRV margin of 1 to 3 mm or vice versa.

It is also worth noting that the EDR relationship of our study is based on the assumption of single target irradiation with the spinal cord in the peripheral dose fall-off region of the target. However, in cases with multiple targets or hypothetical overlapping volumes between the planning target volume

(PTV) and the spinal cord PRV producing focal dose hot spots inside the spinal cord PRV, the formula can deviate significantly from the actual dose limits of such cases so a user should exercise caution for these situations.

In conclusion, a mathematical relationship was found to empirically link the most probable spinal cord PRV dose volume limits across finite isodose volumes such as from Dmax to D(1.0 cc) for common spine SBRT treatments. Further studies are needed to determine general applicability and usefulness of the formula to other SBRT cases.

Comparison of EDR Change Rate for Variable PRVs

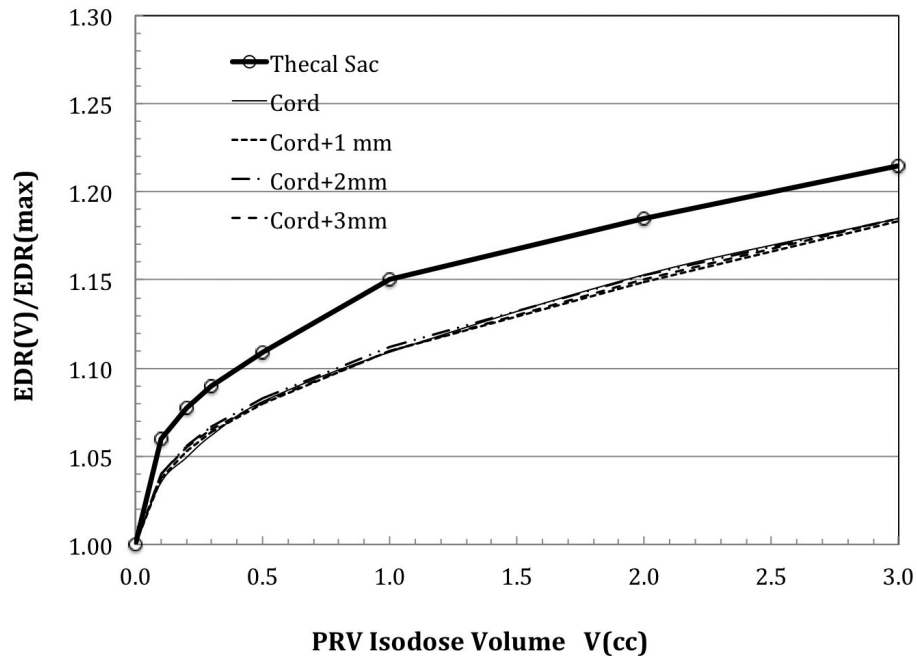


Figure 5. Comparison of the fitted EDR slopes for the studied planning risk volumes (PRVs). Significant differences were noted in the trend of slope changes between the thecal sac and the true cord with and without 1-3 mm margins.

ACKNOWLEDGMENTS

Authors' disclosure of potential conflicts of interest

Dr Sahgal reported grants and an educational honorarium from Elekta AB during the conduct of the study. Drs. Braunstein, Lee, Ma, Soltys, Tseng and Wang have nothing to disclose.

Author contributions

Conception and design: Lijun Ma, Steve Braunstein, Arjun Sahgal

Data collection: Lijun Ma, Lei Wang, Young Lee, Chia-Lin Tseng, Scott Soltys, Steve Braunstein, Arjun Sahgal

Data analysis and interpretation: Lijun Ma, Lei Wang, Young Lee, Chia-Lin Tseng, Scott Soltys, Steve Braunstein, Arjun Sahgal

Manuscript writing: Lijun Ma, Lei Wang, Young Lee, Chia-Lin Tseng, Scott Soltys, Steve Braunstein, Arjun Sahgal

Final approval of manuscript: Lijun Ma, Lei Wang, Young Lee, Chia-Lin Tseng, Scott Soltys, Steve Braunstein, Arjun Sahgal

REFERENCES

1. Chow E, Harris K, Fan G, Tsao M, Sze WM. Palliative radiotherapy trials for bone metastases: a systematic review. *J Clin Oncol.* 2007;25:1423-36.
2. Gerszten PC, Monaco EA, 3rd. Complete percutaneous treatment of vertebral body tumors causing spinal canal compromise using a transpedicular cavitation, cement augmentation, and radiosurgical technique. *Neurosurg Focus.* 2009;27:E9.
3. Gibbs IC, Kamnerdsupaphon P, Ryu MR, Dodd R, Kiernan M, Chang SD, et al. Image-guided robotic radiosurgery for spinal metastases. *Radiother Oncol.* 2007;82:185-90.
4. Guckenberger M, Mantel F, Gerszten PC, Flickinger JC, Sahgal A, Letourneau D, et al. Safety and efficacy of stereotactic body radiotherapy as primary treatment for vertebral metastases: a multi-institutional analysis. *Radiat Oncol.* 2014;9:226.
5. Sahgal A, Ames C, Chou D, Ma L, Huang K, Xu W, et al. Stereotactic Body Radiotherapy Is Effective Salvage Therapy for Patients with Prior Radiation of Spinal Metastases. *Int J Radiat Oncol Biol Phys.* 2009;74:723-31.
6. Sahgal A, Chou D, Ames C, Ma L, Lamborn K, Huang K, et al. Image-guided robotic stereotactic body radiotherapy for

- benign spinal tumors: the University of California San Francisco preliminary experience. *Technol Cancer Res Treat.* 2007;6:595-604.
7. Wang XS, Rhines LD, Shiu AS, Yang JN, Selek U, Gning I, et al. Stereotactic body radiation therapy for management of spinal metastases in patients without spinal cord compression: a phase 1-2 trial. *Lancet Oncol.* 2012;13:395-402.
 8. Yamada Y, Bilsky MH, Lovelock DM, Venkatraman ES, Toner S, Johnson J, et al. High-dose, single-fraction image-guided intensity-modulated radiotherapy for metastatic spinal lesions. *Int J Radiat Oncol Biol Phys.* 2008;71:484-90.
 9. Ma L, Sahgal A, Cozzi L, Chang E, Shiu A, Letourneau D, et al. Apparatus-dependent dosimetric differences in spine stereotactic body radiotherapy. *Technol Cancer Res Treat.* 2010;9:563-74.
 10. Sahgal A, Ma L, Fowler J, Weinberg V, Gibbs I, Gerszten PC, et al. Impact of dose hot spots on spinal cord tolerance following stereotactic body radiotherapy: a generalized biological effective dose analysis. *Technology in cancer research & treatment.* 2012;11:35-40.
 11. Sahgal A, Ma L, Gibbs I, Gerszten PC, Ryu S, Soltys S, et al. Spinal cord tolerance for stereotactic body radiotherapy. *Int J Radiat Oncol Biol Phys.* 2010;77:548-53.
 12. Sahgal A, Larson DA, Chang EL. Stereotactic body radiosurgery for spinal metastases: a critical review. *International journal of radiation oncology, biology, physics.* 2008;71:652-65.
 13. Toussaint A, Richter A, Mantel F, Flickinger JC, Grills IS, Tyagi N, et al. Variability in spine radiosurgery treatment planning - results of an international multi-institutional study. *Radiat Oncol.* 2016;11:57.
 14. Ma L, Sahgal A, Hossain S, Chuang C, Descovich M, Huang K, et al. Nonrandom intrafraction target motions and general strategy for correction of spine stereotactic body radiotherapy. *Int J Radiat Oncol Biol Phys.* 2009;75:1261-5.
 15. Sahgal A, Weinberg V, Ma L, Chang E, Chao S, Muacevic A, et al. Probabilities of radiation myelopathy specific to stereotactic body radiation therapy to guide safe practice. *Int J Radiat Oncol Biol Phys.* 2013;85:341-7.
 16. Gibbs IC. Spinal and paraspinal lesions: the role of stereotactic body radiotherapy. *Front Radiat Ther Oncol.* 2007;40:407-14.
 17. Grimm J, Sahgal A, Soltys SG, Luxton G, Patel A, Herbert S, et al. Estimated Risk Level of Unified Stereotactic Body Radiation Therapy Dose Tolerance Limits for Spinal Cord. *Semin Radiat Oncol.* 2016;26:165-71.
 18. Ryu S, Jin JY, Jin R, Rock J, Ajlouni M, Movsas B, et al. Partial volume tolerance of the spinal cord and complications of single-dose radiosurgery. *Cancer.* 2007;109:628-36.
 19. Sahgal A, Bilsky M, Chang EL, Ma L, Yamada Y, Rhines LD, et al. Stereotactic body radiotherapy for spinal metastases: current status, with a focus on its application in the postoperative patient. *J Neurosurg Spine.* 2011;14:151-66.
 20. Chuang C, Sahgal A, Lee L, Larson D, Huang K, Petti P, et al. Effects of residual target motion for image-tracked spine radiosurgery. *Med Phys.* 2007;34:4484-90.
 21. Foote M, Letourneau D, Hyde D, Massicotte E, Rampersaud R, Fehlings M, et al. Technique for stereotactic body radiotherapy for spinal metastases. *J Clin Neurosci.* 2011;18:276-9.
 22. Ma L, Sahgal A, Descovich M, Cho YB, Chuang C, Huang K, et al. Equivalence in dose fall-off for isocentric and nonisocentric intracranial treatment modalities and its impact on dose fractionation schemes. *Int J Radiat Oncol Biol Phys.* 2010;76:943-8.